International Journal of Geo-Information

MDPI

Article

Machine Learning-Enhanced 3D GIS Urban Noise Mapping with Multi-Modal Factors

Jianping Pan [1,2], Yuzhe He [1], Wei Ma [1,*], Shengwang An [1], Lu Li [1], Dan Huang [1] and Dunxin Jia [3,4]

[1] School of Smart City, Chongqing Jiaotong University, Chongqing 400074, China; panjianping@cqjtu.edu.cn (J.P.); yuzhehe@mails.cqjtu.edu.cn (Y.H.); 622230900018@mails.cqjtu.edu.cn (S.A.); 622230900020@mails.cqjtu.edu.cn (L.L.); 622240101001@mails.cqjtu.edu.cn (D.H.)
[2] Technology Innovation Center for Spatio-Temporal Information and Equipment of Intelligent City, Ministry of Natural Resources, Chongqing 401120, China
[3] School of Architecture and Urban Planning, Chongqing University, Chongqing 400030, China; jiadunxin@caupd.com
[4] China Academy of Urban Planning and Design, Western Branch, Chongqing 401120, China
* Correspondence: weima@cqjtu.edu.cn

Abstract: Geographic Information System (GIS)-based noise management is crucial in urban environments as it provides precise spatial analysis, helping to identify noise hotspots and optimize noise control measures. By integrating noise propagation models with GIS technology, dynamic simulation and visualization of noise distribution can be achieved, offering scientific support for urban planning and noise management. Most existing noise prediction models fail to fully account for three-dimensional (3D) spatial information and a wide range of environmental factors. As a result, there are often discrepancies between the actual noise measurements at monitoring points and the predicted values generated by these models. Furthermore, there is a lack of a system that can effectively integrate noise data with three-dimensional scenes for simulation. This paper proposes a new method to simulate urban noise propagation, aiming to achieve more accurate noise prediction and visualization in a three-dimensional environment. First, we computed the preliminary noise propagation based on a traffic noise model. Next, machine learning techniques were applied to analyze the relationship between noise discrepancies and multi-modal factors, thereby improving the accuracy of environmental noise level estimation. Based on this, we developed an urban noise simulation system. The system integrates functions such as noise simulation, traffic simulation, and weather changes, enabling accurate noise visualization within a three-dimensional virtual environment. Experimental results demonstrate that this method enhances the accuracy of urban noise prediction and visualization, providing users with a more comprehensive understanding of the spatial distribution of urban noise.

Keywords: noise modeling; noise prediction; noise simulation system; machine learning optimization; 3D visualization

check for updates

Academic Editor: Wolfgang Kainz

Received: 7 March 2025
Revised: 6 May 2025
Accepted: 29 May 2025
Published: 4 June 2025

Citation: Pan, J.; He, Y.; Ma, W.; An, S.; Li, L.; Huang, D.; Jia, D. Machine Learning-Enhanced 3D GIS Urban Noise Mapping with Multi-Modal Factors. *ISPRS Int. J. Geo-Inf.* **2025**, *14*, 223. https://doi.org/10.3390/ijgi14060223

Copyright: © 2025 by the authors. Published by MDPI on behalf of the International Society for Photogrammetry and Remote Sensing. Licensee MDPI, Basel, Switzerland. This article is an open access article distributed under the terms and conditions of the Creative Commons Attribution (CC BY) license (https://creativecommons.org/licenses/by/4.0/).

1. Introduction

The acceleration of urbanization has made noise pollution an important issue in urban environmental quality management [1]. Traffic noise, as a major source of urban noise, not only affects the quality of life of residents, but also negatively impacts public health and urban ecosystems [2–7]. Geographic Information Systems are essential tools in noise research, widely used for noise data collection, analysis, and visualization [8]. Compared to traditional field measurements, GIS technology enables more efficient processing of large-scale spatial data and provides a more comprehensive assessment of noise pollution [9,10].

GIS tools can integrate spatial data such as road networks, building layouts, and terrain features while incorporating machine learning and big data techniques to optimize noise prediction models and improve the accuracy of noise assessments [11–14].

The World Health Organization (WHO) has proposed a series of recommendations to mitigate the impact of noise pollution, including establishing strict environmental noise standards, optimizing urban traffic planning, improving building sound insulation measures, and raising public awareness of noise protection [15]. The complex topography of mountainous cities further exacerbates the complexity of noise propagation and creates higher requirements for noise prediction and management [16]. Many studies have been conducted on the propagation law and influencing factors of traffic noise, and noise prediction methods based on statistical and physical models have been developed [17,18]. These methods are usually calculated with traffic flow, vehicle type, and speed as the core parameters [19–21]. In addition, machine learning algorithms based on statistical models are gradually used for environmental noise prediction [22,23]. However, these techniques still face the problems of low prediction accuracy and low computational efficiency when dealing with large-scale complex scenes. Meanwhile, with the rapid development of virtual reality technology, research on combining 3D visualization with noise simulation has begun to receive attention [24]. In the field of data science, "multi-modal" typically refers to data of different types or varying formats within the same data type [25]. In this study, the multi-modal factors mainly include heterogeneous data such as road networks, traffic flow, topography, and vegetation. Effectively integrating these multi-modal datasets helps to achieve a more comprehensive understanding of the relationship between environmental noise levels and influencing factors. However, the ability of existing systems to integrate multi-modal data and realize dynamic visualization still needs to be improved.

To address the challenges mentioned above, this study proposes an innovative technical framework that combines advanced noise propagation models with machine learning optimization techniques, enabling accurate noise prediction and intuitive visualization of its distribution. By integrating multi-source data such as topography, vegetation, and road networks, we have enhanced the accuracy of noise prediction. Building on this, we developed an urban noise simulation system based on Unreal Engine (UE), allowing users to intuitively understand and analyze noise distribution in urban environments

Our contribution can be summarized as follows:

- We propose a multi-source data fusion approach for noise prediction, integrating topography, vegetation, road network data, and utilizing machine learning optimization techniques to improve prediction accuracy.
- We present a technical solution for simulating noise propagation in the complex environment of mountainous cities, combining noise propagation models with machine learning techniques, and developing an urban noise simulation system integrated with 3D scenes, providing scientific support and visualization for urban noise management and decision-making.

The organizational structure of this article is as follows. Section 2 reviews the relevant work. Section 3 introduces the main methods. Section 4 describes the study area and discusses the experimental results. Section 5 provides conclusions and recommendations for future work.

2. Related Work

Most strategic noise mapping relies on standardized methods, and the introduction of Geographic Information Systems has significantly improved the efficiency of this process, as noise mapping requires the processing of large amounts of spatial data [26]. GIS tools were first applied to environmental noise prediction studies back in 1997, which analyzed

the effects of widespread road traffic noise on breeding birds in the Netherlands [27]. As research has progressed, the combination of field measurements and interpolation techniques has been proven effective in capturing the spatial distribution characteristics of noise pollution. For example, Shim et al. [28] utilized participatory noise data and applied the inverse distance weighted (IDW) interpolation method to create a detailed noise map of Seoul, illustrating temporal variations in noise levels. This approach provided a more comprehensive understanding of urban noise pollution patterns. Similarly, Avgoustina et al. [8] measured noise levels in the historical center of Athens from May to August 2021 and employed the Kriging spatial interpolation method to generate a noise-distribution map for the study area. However, these methods are limited by the difficulty of data acquisition, as the accuracy of interpolation depends on the distribution of monitoring points and involves high computational costs, which affect the applicability of noise prediction.

Multiple linear regression models have been widely used in the field of traffic noise prediction, including the FHWA model in the United States [29], the CoRTN model in the United Kingdom [30], the RLS90 model in Germany [31], the ASJ RTN-Mode model in Japan [32], the CNOSSOS-EU model in Europe [33], and the NMPB-08 prediction method in France [34]. In addition, China's Technical Guidelines for Noise Impact Assessment (HJ 2.4-2009) [35] provide a standardized methodology for noise prediction [36]. These types of numerical simulation methods have long been the standard approach in noise research. However, due to their limited consideration of environmental factors, machine learning algorithms have demonstrated significant advantages in noise prediction in recent years. With their strong capability to capture complex nonlinear relationships, they have gradually become a vital research tool in this field. Among these, artificial neural networks (ANN), as a powerful statistical learning tool, have been increasingly applied in the field of road traffic noise prediction [37–39]. These studies generally consider traffic volume, the proportion of heavy vehicles, and average vehicle speed as key input parameters for constructing neural network models. Liu et al. [40] proposed a hybrid noise mapping method that combines a traffic noise propagation model with the random forest (RF) algorithm to generate environmental noise maps for multiple time periods across the Island of Montreal, Canada, demonstrating the effectiveness and feasibility of the hybrid model for large-scale environmental noise estimation. Other studies have employed forward stepwise regression to establish relationships between noise levels and predictor variables [41,42]. For example, the study by Xu et al. [43] validated the reliability of this method in modeling noise variability in megacities such as Shanghai, achieving a model accuracy of 0.79. Almansi et al. [14] developed three models—random forest, gradient boosting (GB), and extreme gradient boosting (XGB)—to predict traffic noise levels on a university campus, and demonstrated that the XGB model outperformed the other two across multiple performance metrics. Furthermore, deep learning methods, such as convolutional neural networks (CNN) [44] and long short-term memory (LSTM) networks [45], have achieved promising results in spatiotemporal noise prediction. These algorithms offer significant advantages in noise exposure modeling, particularly in analyzing spatial variability. However, there are still limitations in current research, such as the absence of complete system construction and the lack of visualization analysis in a three-dimensional environment.

Among others, one study developed an integrated GIS system suitable for traffic noise prediction in China and implemented the model based on the commercial GIS software ArcView (now ArcGIS) [46]. In addition, the open-source application SPreAD-GIS was designed to model anthropogenic noise propagation in natural ecosystems and was written in Python and implemented as a toolbox in ArcGIS 9.3 [47]. Similarly, Gulliver et al. [48] developed an open-source tool for modeling traffic noise in ArcGIS in 2015. Meanwhile, academic open-source tools such as NoiseModelling and OpeNoise provide specialized

noise mapping programs [49–51]. NoiseModelling proposed a framework that integrates a simplified noise modeling approach into GIS software as a service module, enabling efficient processing of large volumes of input and output data. Recently, Ascari et al. [52] introduced the OUTFIT project, which extends beyond traditional GIS-based models by incorporating crowdsourced traffic data, real-time data stream optimization, and 3D rendering into a Digital Twins framework for dynamic road traffic noise mapping. This system enables more flexible, data-driven decision-making and offers new possibilities for integrating perception-based and model-based noise evaluation. Nonetheless, the application of these methods in complex terrains, especially in mountainous cities, still faces limitations in terms of accuracy and applicability.

In the field of 3D visualization technology, Unreal Engine has established a significant presence in digital twin applications due to its physically accurate rendering pipeline. Originally developed for real-time 3D game rendering, UE is now widely used as a general-purpose platform for interactive simulations across disciplines. This platform leverages a C++-based architecture combined with a Blueprint visual scripting system to create a hybrid development framework that supports augmented reality environments. Its rendering core utilizes ray tracing technology and optimized particle systems to realistically simulate complex visual elements such as dynamic lighting and volumetric fog effects [53,54]. It is worth noting that although Unreal Engine has established a mature application paradigm in Building Information Modeling (BIM) visualization, research on integrating its high-performance rendering capabilities with acoustic propagation models remains in the exploratory stage. At present, although Unreal Engine has seen limited use in simulating urban noise propagation, this study explores its potential as a visualization platform for acoustic data, leveraging its rendering capabilities to represent complex environmental sound fields in an interactive way. Rian [55] demonstrated the feasibility of using the commercial game engine UE in acoustic simulation, breaking away from traditional custom software development models. This significantly reduces the technical barriers and labor costs associated with professional acoustic modeling. However, the lack of validation with real-world data for multi-scale scenarios and the absence of quantitative evaluation metrics for acoustic simulation accuracy limit its broader application in more complex environments.

3. Materials and Methods

3.1. Overview

In this study, we aim to develop an urban noise simulation system with the technical framework shown in Figure 1. The main work is divided into three parts: pre-noise map construction by traffic noise propagation model, multi-modal factors-driven noise optimization, and noise propagation simulation in complex scenarios.

As shown in Figure 1, we first collected data on noise level, traffic flow, topographic features, and building distribution in the area to provide comprehensive data support for the study. Then, the CNOSSOS-EU traffic noise propagation model was used to calculate the distribution of traffic noise in the study area, and the discrepancies between the theoretically calculated and measured values were obtained by comparing the theoretically calculated and measured values at the monitoring points. Based on this, the relationship model between the noise discrepancies and the multi-modal factors was established using the machine learning method of ridge regression. On this basis, an urban noise simulation system based on Unreal Engine 5 was developed. The system integrates the functions of noise simulation, traffic flow dynamic simulation, and high-precision 3D scene loading, and realizes the intuitive visual expression of urban noise propagation.

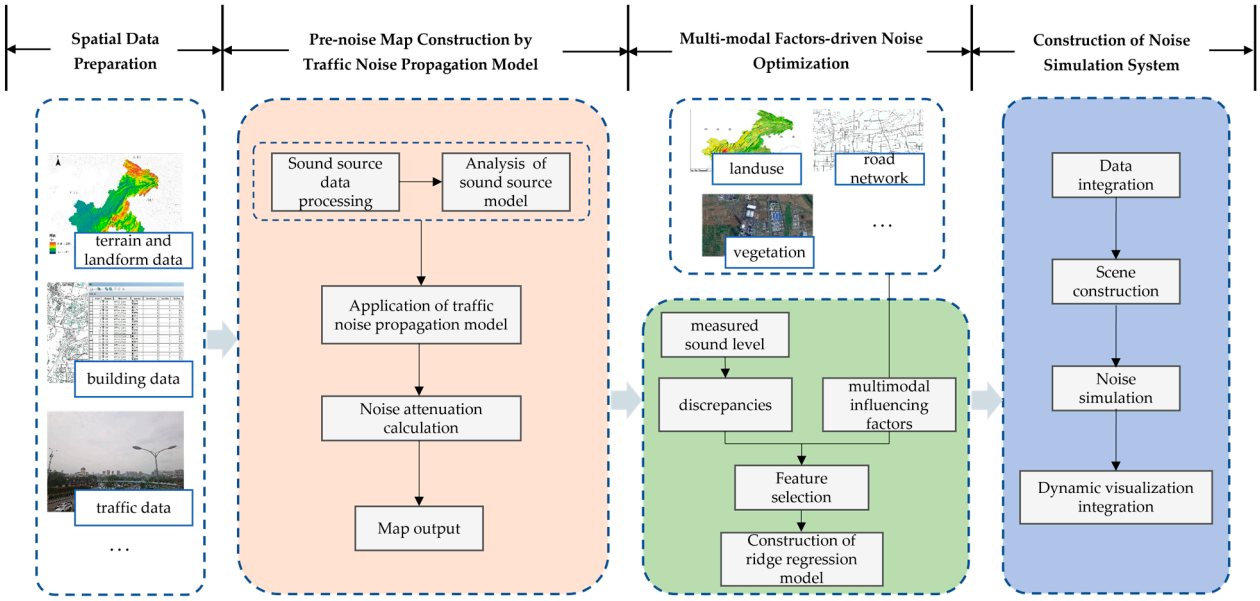


Figure 1. The technical framework of the study.

3.2. Pre-Noise Map Construction by Traffic Noise Propagation Model

The traffic noise propagation model simulates how noise travels within a specified physical environment, accounting for processes such as surface reflections and ground effects. This study utilizes the vehicle noise emission, attenuation, and reflection standards outlined in CNOSSOS-EU. During the propagation of sound from the source to the receiver, factors such as geometric spreading, air absorption, ground interactions, and obstacles result in various types of attenuation. To ensure accurate modeling, corrections must be applied to account for these influencing factors throughout the propagation process [56].

Assuming traffic data as the sole source of noise emissions, there are multiple propagation paths from the sound source to the receiver, including four main types: direct sound, reflected sound, diffracted sound, and mixed path. Equations (1)–(5) [57] constitute the core components of the traffic noise propagation process. Different propagation paths result in varying degrees of attenuation, and the sound level after accounting for these types of attenuation can be expressed as follows:

$$L = L_W - A \tag{1}$$

where L_W is the source noise and A is the sum of the attenuation in the propagation process, the specific expression is:

$$A = A_{div} + A_{atm} + A_{boundary,F} \tag{2}$$

where A_{div} is the attenuation due to geometric dispersion, A_{atm} is the attenuation due to air absorption, and $A_{boundary,F}$ is the attenuation due to changes in boundary conditions, including ground effect A_{grd} and various types of diffractions A_{dif}.

The geometric dispersion is related to the distance d between the sound source and the receiver, and is given by:

$$A_{div} = 20\log_{10}(d) + 11 \tag{3}$$

The air absorption is related to the distance d and the atmospheric absorption coefficient α_{atm} by the expression:

$$A_{atm} = \alpha_{atm}\frac{d}{1000} \tag{4}$$

The ground effect is primarily caused by the attenuation resulting from the interference between reflected sound and direct sound. When diffraction is included in the calculation, the ground effect is not considered separately. The expression for diffraction sound attenuation is:

$$A_{dif} = \Delta_{dif(S,R)} + \Delta_{ground(S,O)} + \Delta_{ground(O,R)} \quad (5)$$

where $\Delta_{dif(S,R)}$ represents the diffraction attenuation between the sound source and the receiver, $\Delta_{ground(S,O)}$ denotes the attenuation caused by ground effects between the sound source and the diffraction point, and $\Delta_{ground(O,R)}$ indicates the attenuation caused by ground effects between the diffraction point and the receiver.

3.3. Multi-Modal Factors-Driven Noise Optimization

There are certain discrepancies (denoted as D_{tnpm}) between the calculated values of the traffic noise propagation model (denoted as L_{tnpm}) and the measured sound levels (denoted as $L_{measure}$) at monitoring points, and these discrepancies are related to the surrounding environment. To capture this relationship, a ridge regression method is employed to construct a mapping between the noise discrepancies and multi-modal factors. By combining the prediction results of the ridge regression model (denoted as D_{ridge}) with L_{tnpm}, an optimized noise model (denoted as L_{env}) was developed, producing results closer to the measured values.

The entire process consists of two main steps: first, key features are selected using the forward stepwise regression method [58]; and second, a prediction model is developed using ridge regression to accurately describe this relationship.

The model was evaluated using five-fold cross-validation to assess its stability and generalization ability. In each cross-validation iteration, the dataset was divided into multiple subsets. The model was trained and tested on different subsets in sequence, and the average performance metrics were calculated to mitigate overfitting risks. Five-fold cross-validation was selected as it provides a suitable trade-off between computational efficiency and robustness in performance evaluation, particularly for datasets of moderate size as used in this study. Compared to three- or ten-fold alternatives, five-fold cross-validation yielded relatively stable performance estimates with acceptable variance during preliminary analyses. The predictive performance of the model was assessed using multiple metrics, including the coefficient of determination (R^2), mean error (ME), root mean square error (RMSE), and mean absolute error (MAE) [59–61]. These metrics quantified the accuracy of the predictions. Additionally, a comparison chart between the predicted values from the ridge regression model (D_{ridge}) and D_{tnpm} was plotted to further validate the model's predictive ability and consistency.

3.3.1. Feature Selection

To control model complexity and mitigate the impact of redundant variables on regression performance, this study employed forward stepwise regression based on ordinary least squares (OLS) for feature selection. This method iteratively constructs the regression model by introducing explanatory variables with the strongest predictive power, using statistical significance as the inclusion criterion [62]. The algorithm starts with an initial model containing only the intercept term. In each iteration, it evaluates all candidate variables not yet included in the model by computing the t-statistics of their regression coefficients, which reflect the explanatory strength of each variable. The t-statistic is calculated as:

$$t_j = \frac{\hat{\beta}_j}{SE(\hat{\beta}_j)} \quad (6)$$

where $\hat{\beta}_j$ represents the regression coefficient, and $SE(\hat{\beta}_j)$ is the standard error of the regression coefficient. The corresponding p-value is used to assess statistical significance. A variable is included in the model only if its p-value is below a pre-specified threshold, set at 0.05 in this study.

Model parameters are estimated by minimizing the Residual Sum of Squares (RSS), calculated as follows:

$$RSS = \sum_{i=1}^{n} (y_i - \hat{y}_i)^2 \tag{7}$$

In this formula, y_i represents the true value of the i-th sample, and $\hat{y}_i$ is the predicted value based on the current model. The iterative process continues until no additional variable satisfies the significance criterion. The final regression model takes the following form:

$$Y = \beta_0 + \sum_{j=1}^{m} \beta_j X_j + \varepsilon \tag{8}$$

In this model, Y represents the target variable, X_j denotes the selected features,β_0 is the intercept term, β_j is the regression coefficient for the corresponding feature, and ε is the error term. In this way, forward stepwise regression can effectively select the most relevant variables from a large number of candidate features, thereby improving the prediction accuracy and interpretability of the regression model.

3.3.2. Ridge Regression Analysis

Ridge regression is suitable for collinearity data analysis and regression model construction [63,64]. Therefore, ridge regression was used to build the noise discrepancy prediction model. When dealing with collinear data, the ridge regression method abandons the unbiasedness of the least squares method. By sacrificing some information and reducing accuracy, it produces regression coefficients that are more realistic and reliable. Its fitting performance on multicollinear data is superior to that of the least squares method.

The solution method of the least squares model is based on the concept of minimizing the mean squared error (MSE). The core idea is to find a fitting line that minimizes the total variance between the sample points and the line. The calculation formulas for ordinary least squares are shown in Equations (9) and (10).

$$\mathbf{Y} = \mathbf{W}^T \mathbf{X} \tag{9}$$

$$\mathbf{W} = (\mathbf{X}^T \mathbf{X})^{-1} \mathbf{X}^T \mathbf{Y} \tag{10}$$

The ridge regression algorithm improves accuracy by sacrificing some information, a process in which a penalty term α for the regression coefficients is added to the least squares model. If α increases, the degree of contraction increases accordingly, which makes the model more unbiased and effectively reduces its error. On the contrary, if α decreases, the gap between predicted results and the real data becomes smaller, while the degree of contraction decreases. When α is 0, the model becomes the least squares method. Therefore, α should be chosen as the minimum value that satisfies the requirements of the study.

$$\mathbf{W} = (\mathbf{X}^T \mathbf{X} + \alpha \mathbf{I})^{-1} \mathbf{X}^T \mathbf{Y} \tag{11}$$

In this formula, $\mathbf{I}$ is the identity matrix.

3.4. Construction of Noise Simulation System

Building upon the outputs of the traffic noise propagation model (Section 3.2) and the optimized environmental noise predictions (Section 3.3), this section presents the

implementation of a comprehensive urban noise simulation system. The system uses the optimized noise levels (L_{env}) as input and integrates them with 3D spatial scene data within Unreal Engine to support immersive and realistic visualization. Figure 2 illustrates the overall framework of the proposed system. Specifically, Figure 2a shows the system architecture diagram, which outlines the structure of the data layer, technical support layer, and application layer. Figure 2b presents the data flow diagram, detailing how key outputs—L_{tnpm}, D_{ridge}, and L_{env}—are transferred and processed across different modules to generate 3D urban noise simulations.

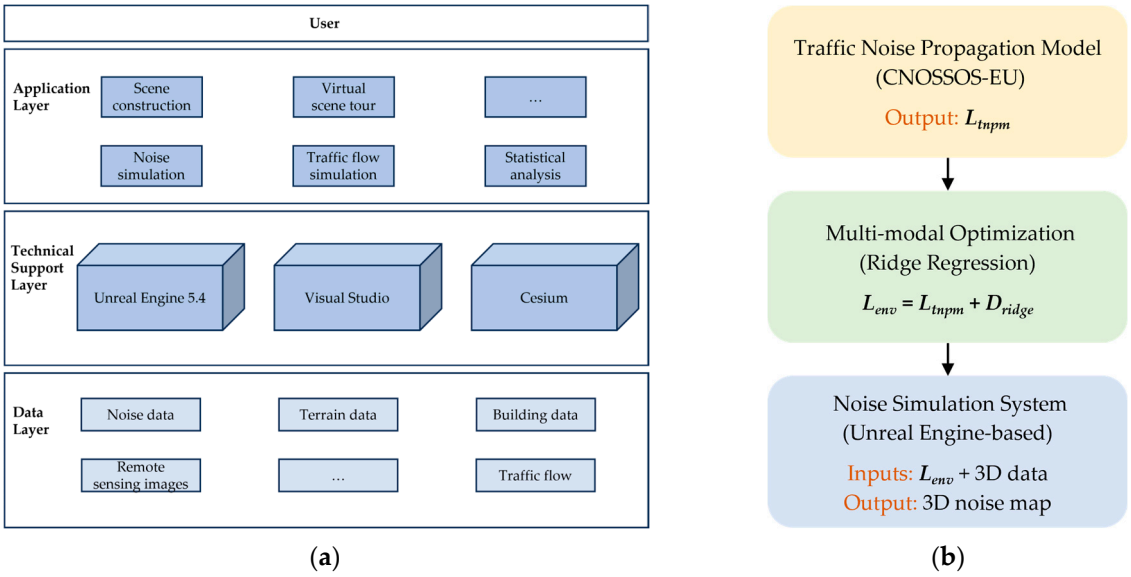


Figure 2. Overall architecture and data flow of the urban noise simulation system. (**a**) System architecture diagram; (**b**) Data flow diagram.

First, the real-world scene data collected using Light Detection and Ranging (LiDAR) and oblique photography technology is imported into the Unreal Engine 5 editor. A unified spatial reference coordinate system is established to ensure data consistency and importability. The terrain is then smoothed using UE tools, and simulation details are added to enhance the realism of the scene. To improve rendering performance, Level of Detail (LOD) technology is applied to layer scene elements such as buildings and terrain, and lighting settings are optimized to strike a balance between rendering quality and performance, ultimately creating a highly realistic virtual scene.

In terms of noise simulation, GeoJSON geographic data is converted to a compatible format, allowing the noise field to be recognized and loaded by Unreal Engine. This involves the following steps: (1) the GeoJSON file is read to extract polygon geometries and their corresponding noise level attributes (ISOLVL). Invalid geometries, such as self-intersections or unclosed rings, are corrected using a buffer(0) operation to enforce topological validity; (2) the spatial extent of the feature is calculated based on the minimum bounding rectangle (MBR), and the raster resolution (rows and columns) is determined dynamically according to a fixed pixel size; (3) the rasterio library is used to rasterize the vector polygons into a noise intensity grid, in which the minimum ISOLVL value is retained in overlapping areas; (4) ISOLVL values are linearly normalized to a grayscale range of 0–255, and Gaussian blur is applied to smooth edges and artifacts, enhancing visual continuity; and (5) the processed raster is exported in BMP format as a grayscale height map for 3D mesh terrain modeling. In terms of height map processing, detailed optimization is performed on the fluctuations of the noise field's elevation to more realistically simulate

noise intensities. Additionally, textures are applied to the surface materials of the noise field, making the simulated noise environment visually more realistic.

The noise simulation results are dynamically integrated with the virtual scene by using Unreal Engine's real-time fusion technology. Through the blueprint design tool in Unreal Engine, the noise simulation data is dynamically linked to the properties of scene elements, allowing for real-time adjustments of noise field colors and intelligent parameter associations, thereby enhancing the realism of the simulation. A particle system is employed to enhance the visual effects of noise within the virtual environment, and the scene's lighting setup is optimized based on noise propagation characteristics. This process establishes a light-responsive mechanism: higher noise levels result in warmer and more intense lighting, whereas lower noise levels produce cooler and dimmer illumination, further improving the overall realism of the scene.

4. Results

4.1. Study Area

Chongqing, located in southwestern China, is characterized by mountainous and hilly terrain with diverse urban landforms. This study focuses on the area along both sides of the inner ring viaduct from Wujiang Interchange to Donghuan Interchange in Yubei District, Chongqing, covering a total area of approximately 35.8 km^2. This region includes two major transportation hubs, Beihuan Interchange and Renhe Interchange (as shown in Figure 3). With heavy traffic flow and densely distributed buildings, the area comprehensively reflects the impact of complex urban terrain and diverse environmental conditions on urban noise patterns.



Figure 3. Overview of the study area.

4.2. Data Collection

From 6:00 a.m. on 7 May 2024, to 6:00 a.m. on 8 May 2024, noise monitoring was conducted at 60 locations [65]. The noise monitoring equipment included the AWA6228 and AWA6228+ sound level meters, which were acoustically calibrated with a calibration error of less than $\pm$0.5 dB. Following the standards outlined in the Technical Specifications for Environmental Noise Monitoring, Routine Monitoring for Urban Environmental Noise (HJ 640-2012) [66], the noise levels at each point were measured for 1 h, ensuring at least four complete sets of noise monitoring experiments per point. The sound level meters were mounted on tripods at each monitoring point and positioned at a height of 1.5 m above the ground. To minimize noise reflection, the meters were placed at least 2 m away from potential sound barriers. The coordinates of each point were determined and recorded

using Google Maps. As shown in Figure 4, the collected data were used for subsequent noise analysis and modeling.

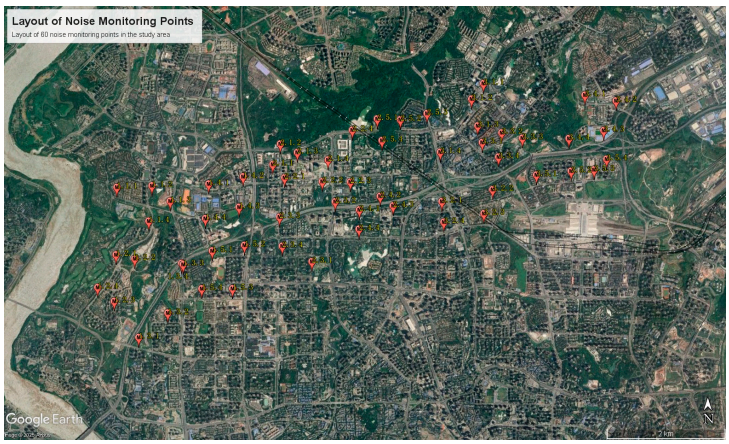


Figure 4. Layout of monitoring points.

Road traffic noise is produced by various types of vehicles in the traffic flow. During the monitoring period, traffic data such as traffic volume, vehicle types, and driving speeds were collected through the playback of the Chongqing Traffic Management Bureau's video surveillance system. This data helped to analyze traffic conditions across different time periods and road sections. The average driving speed of vehicles is classified based on the road's speed limits.

The Digital Elevation Model (DEM) was derived from the Advanced Land Observing Satellite (ALOS) data released by the Japan Aerospace Exploration Agency in 2019, with a spatial resolution of 12.5 m. Vector data containing building heights and outlines were provided by the Chongqing Academy of Surveying and Mapping, serving as a crucial input for constructing the traffic noise propagation model.

4.3. Traffic Noise Propagation Model Noise Estimation

In this study, we conducted a comparative analysis between the measured sound levels ($L_{measure}$) at monitoring points and the predicted values derived from the traffic noise propagation model (L_{tnpm}). In this study, $L_{measure}$ refers to the arithmetic mean of noise measurements taken at multiple time intervals between 6:00 and 18:00, representing the actual noise level during this period. L_{tnpm} denotes the equivalent continuous sound level predicted for the entire daytime period defined as 6:00 to 18:00. Table 1 provides a statistical summary of the measured sound levels and the predicted values of the traffic noise propagation model at monitoring points within the study area.

Table 1. Statistical summary of $L_{measure}$ and L_{tnpm} at monitoring points.

	$L_{measure}$ (dB(A))	L_{tnpm} (dB(A))
Mean	61.23	74.77
Median	62.70	76.31
SD [1]	4.87	10.41
Minimum	50.90	50.64
Maximum	68.75	91.02

[1] stands for standard deviation.

The statistical analysis of $L_{measure}$ shows that the average sound level at the monitoring points is 61.23 dB(A), with a median of 62.7 dB(A). The standard deviation is 4.87 dB(A), indicating a certain degree of fluctuation around the mean. The minimum recorded value

is 50.9 dB(A), while the maximum reaches 68.75 dB(A). In comparison, the mean value of L_{tnpm} is 74.77 dB(A), which is significantly higher than the measured mean of 61.23 dB(A), resulting in a difference of approximately 14 dB(A). The median of L_{tnpm} is 76.31 dB(A), with a standard deviation of 10.41 dB(A), showing greater variability in the predictions. The minimum value of L_{tnpm} is 50.64 dB(A), and the maximum reaches 91.02 dB(A), suggesting a significantly broader range and greater variability in the predicted results.

The MAE is 13.96 dB(A), reflecting the average deviation between L_{tnpm} and $L_{measure}$. The RMSE is 16.14 dB(A), further illustrating the overall fluctuation of the prediction errors.

4.4. Noise Optimization

This study selected key factors influencing noise propagation, including traffic volume, road networks, slope, and the Normalized Difference Vegetation Index (NDVI). A raster map with a spatial resolution of 30 m × 30 m was constructed, and each raster cell was assigned values based on the following criteria: (1) the distance from the cell center to the nearest road; (2) the total road length and traffic volume within specific buffer zones (50 m, 100 m, 150 m, 200 m, 250 m, 300 m, 400 m, and 500 m); and (3) the NDVI value and slope at the cell center. The generated raster map was used as a set of candidate predictor variables for the model. Predictor variables corresponding to monitoring points were extracted based on their latitude and longitude. The discrepancies (D_{tnpm}) between $L_{measure}$ and L_{tnpm} at monitoring points were computed, forming a complete dataset. A total of 53 samples and 36 feature variables were obtained.

A forward stepwise regression method was applied to select relevant features from the initial set of 36 candidate variables. This approach iteratively introduces predictors into the model based on their statistical significance (p-values) under an OLS regression framework, retaining only those variables with $p < 0.05$ until no further significant variables remain. The goal was to identify variables with a statistically significant association with the target variable D_{tnpm}. After feature selection, a regularized regression model was used for training.

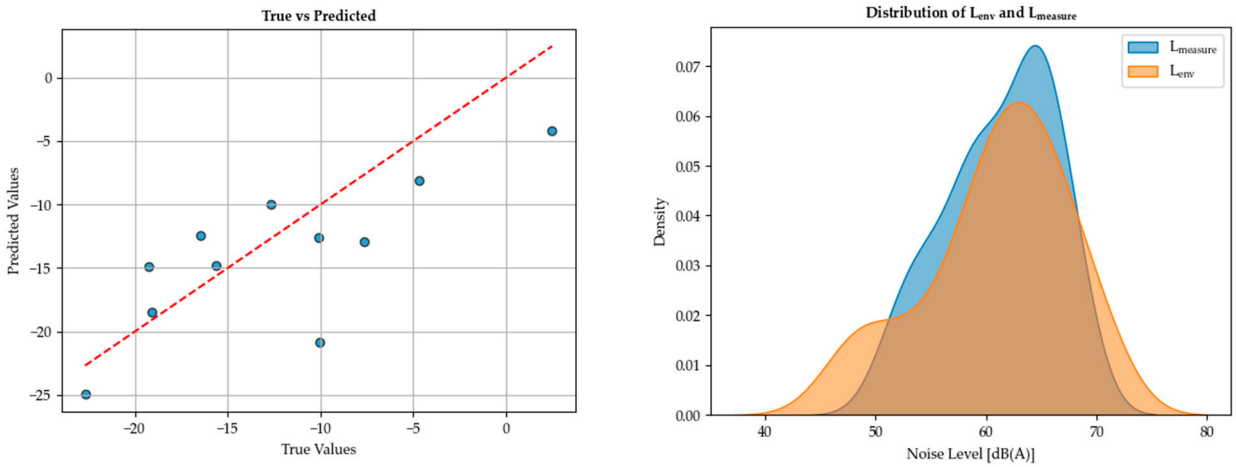
The stepwise procedure identified three statistically significant predictors of D_{tnpm}, all of which satisfied the significance criterion during model fitting: the number of light-duty vehicles within a 150 m buffer (LVD150), the number of light motorcycles within a 50 m buffer (WAVD50), and the total road length within a 100 m buffer (len100). Table 2 shows the results of the final regression model based on predictors selected via forward stepwise regression. The coefficients (coef.) indicate the change in D_{tnpm} per unit increase in each predictor variable. The model trained on these features achieved an R^2 of 0.53 on the test set. Further evaluation showed that the MSE was 23.18, the RMSE was 4.81, and the MAE was 3.95, reflecting the magnitude of prediction errors. The five-fold cross-validation results indicated an average R^2 of 0.43 with a standard deviation of 0.18, suggesting moderate generalization ability.

Table 2. Results of the final regression model based on predictors selected via forward stepwise regression (R^2 = 0.527).

Variable Name	Unit of the Coef. and the (95% CI)	Coef.	(95% CI)	*p*-Value
LVD150	# [1]	−5.747	(−7.659, −3.835)	<0.001
WAVD50	#	−3.212	(−5.100, −1.323)	0.001
len100	m	−2.760	(−4.697, −0.822)	0.006

[1] stands for quantity (number of items).

Figure 5a presents a scatter plot of D_{ridge} and D_{tnpm} to evaluate the model's fitting performance. The results show a certain correlation between D_{ridge} and D_{tnpm}, but some deviations remain. This may be due to the limited size of the data sample.



(**a**) (**b**)

Figure 5. Accuracy evaluation of noise optimization. (**a**) Scatter plot of D_{ridge} (Predicted Values) vs. D_{tnpm} (True Values). Each dot represents a test sample. The red dashed line denotes the ideal line where predicted values equal true values; (**b**) Distribution of L_{env} and $L_{measure}$.

The predicted noise discrepancies derived from the ridge regression model (D_{ridge}) were added to the predicted results of the traffic noise propagation model (L_{tnpm}) to obtain the total environmental noise (L_{env}), which is closer to the measured sound levels.

Figure 5b compares the distribution characteristics of $L_{measure}$ and L_{env} at noise monitoring points. The horizontal axis represents the noise level range, while the vertical axis indicates data density. The figure shows that both curves peak around 60 dB(A), suggesting that this noise level occurs most frequently in both the measured data and the environmental noise prediction results. And the two distributions exhibit a similar pattern, forming a bell-shaped curve with higher density in the middle and lower density at both ends. Within the range of 45–75 dB(A), the density distribution is relatively concentrated, whereas noise levels outside this range occur with lower probability. The chart uses color differentiation to clearly distinguish the data categories, making the correspondence between L_{env} and $L_{measure}$ in terms of intensity distribution more intuitive.

Table 3 provides a statistical summary of the measured sound levels and total environmental noise predictions at monitoring points within the study area.

Table 3. Statistical summary of $L_{measure}$ and L_{env} at monitoring points.

	$L_{measure}$ (dB(A))	L_{env} (dB(A))
Mean	61.23	60.96
Median	62.70	62.50
SD [1]	4.87	6.38
Minimum	50.90	45.93
Maximum	68.75	71.30

[1] stands for standard deviation.

This study compares the statistical characteristics of L_{env} and $L_{measure}$. The mean value of L_{env} is 60.96 dB(A), which is very close to the mean of $L_{measure}$ at 61.23 dB(A). The median of L_{env} is 62.50 dB(A), slightly lower than the median of $L_{measure}$ at 62.7 dB(A). The standard deviation of L_{env} is 6.38 dB(A), slightly lower than that of L_{tnpm}, indicating that

the optimized model exhibits less fluctuation in predictions. The minimum and maximum values of L_{env} are 45.93 dB(A) and 71.30 dB(A), respectively, showing a narrower range than before optimization.

Error analysis indicates a significant improvement in prediction accuracy after optimization. The ME is 0.28 dB(A), a substantial reduction compared to −13.54 dB(A) before optimization. The MAE is 4.57 dB(A), approximately two-thirds lower than the pre-optimization value of 13.96 dB(A), indicating a significant reduction in the deviation between predicted and measured values. The RMSE decreased from 16.14 dB(A) to 5.67 dB(A), further demonstrating the improved predictive accuracy of the optimized model.

As shown in Figure 6, the optimized noise model (L_{env}) provides a more realistic spatial representation of urban noise distribution. While its general spatial pattern remains similar to that derived from the initial traffic noise propagation model (L_{tnpm}), the L_{env} predictions exhibit reduced overestimation and improved agreement with measured values, particularly in areas with heavy traffic such as major and secondary roads. However, since the propagation model primarily estimates noise based on road networks with traffic volume, and the selected predictor variables are closely related to roads and traffic intensity, noise levels tend to be underestimated in areas that are distant from or poorly connected to the road network.



Figure 6. Spatial distribution of noise levels predicted by the optimized model (L_{env}).

4.5. Noise Propagation Simulation

The system successfully integrates and implements multiple functions within a virtual environment, providing a comprehensive and intuitive analytical tool for urban noise research.

Figure 7 illustrates selected functionalities of the urban noise simulation system: (a) A real-world 3D model of the study area, constructed from LiDAR point clouds and oblique photogrammetry data, is loaded into a true-georeferenced coordinate system. The model features rich detail, with terrain undulations and building outlines accurately reproduced, providing a close match to the actual environment and enhancing spatial perception and immersion. (b) Noise simulation data is overlaid onto the real-world model: red areas represent high noise intensity, while blue areas indicate low intensity. The noise distribution is clearly distinguishable, highlighting noise hotspots along roads and critical nodes, offering valuable decision support for noise mitigation and urban planning. (c) A dynamic traffic flow visualization, based on measured traffic volume data, simulates vehicles as traffic streams moving in real-time through the 3D scene, illustrating variations in traffic density over time. The smooth and natural rendering of vehicle movement

aids in the analysis of congestion hotspots and the optimization of traffic management. (d) The system's statistical analysis dashboard includes three panels on the left: (1) a radar chart displaying noise distribution in different directions across various time intervals, (2) a noise-trend analysis chart showing temporal variations in noise intensity for a selected area, and (3) a noise-curve fitting plot to assess noise propagation patterns. On the right, the panels show: (1) comparative noise-distribution maps for different subregions and time periods, (2) aggregated noise statistics for each subregion, and (3) a time-series chart for traffic volume. This comprehensive and interactive module enables multidimensional, detailed assessments of environmental noise and traffic flow.

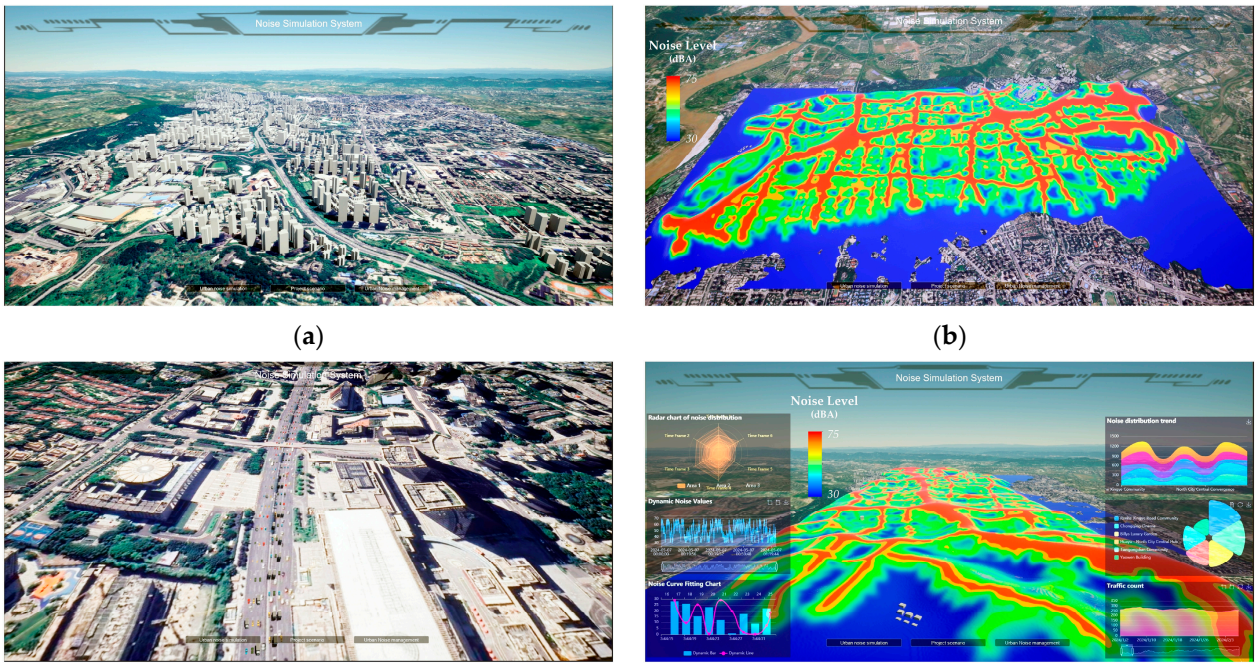


Figure 7. Functions of the urban noise propagation simulation system. (**a**) Scene construction; (**b**) Noise simulation; (**c**) Traffic flow simulation; (**d**) Statistical analysis.

5. Conclusions and Future Work

The work presented in this study aims to develop a system that integrates urban noise simulation, dynamic visualization, and multi-functional capabilities, significantly improving prediction accuracy through model optimization. By combining 3D scene data with efficient algorithms, we simulate the distribution of noise in urban environments. This provides new technical support for the study of noise behavior in complex urban settings. The core function of the system is urban noise simulation. By integrating GeoJSON-format geographic data with the rendering power of Unreal Engine, the system accurately represents the spatial distribution of noise in three-dimensional space. To address data gaps, Gaussian blur techniques were applied to ensure the integrity and continuity of the noise field. The optimized noise field not only presents a more detailed spatial distribution but also reflects the real changes in noise intensity, enhancing the credibility of the simulation. In addition, a large number of field noise measurements were conducted in this study to support model training and evaluation. This extensive dataset contributed significantly to improving the accuracy and robustness of the noise prediction model. One of the advantages of our system is its ability to efficiently integrate urban noise simulation with traffic and weather changes while significantly reducing prediction errors. This makes the

urban noise simulation system more accurate and adaptable, providing effective technical support for urban environmental noise management.

Future research could expand the scope of data collection to include a wider range of scenes and environmental conditions to verify the model's applicability. To improve computational efficiency, more efficient methods could be explored, and the complexity of the current model could be optimized. Additionally, further investigation into the impact of environmental factors on noise propagation, particularly by incorporating more detailed terrain and building data, could enhance the realism of simulation results. The findings of this research can be integrated with urban management to develop decision support tools, offering technical support for noise control.

Author Contributions: Conceptualization, Jianping Pan, Yuzhe He, and Wei Ma; methodology, Yuzhe He; data acquisition, Yuzhe He, Shengwang An, Lu Li, and Dan Huang; software, Yuzhe He and Shengwang An; writing—original draft, Yuzhe He; writing—review and editing, Jianping Pan, Yuzhe He, and Wei Ma; project administration, Jianping Pan and Wei Ma; funding acquisition, Jianping Pan, Wei Ma, and Dunxin Jia. All authors have read and agreed to the published version of the manuscript.

Funding: This research was funded by the Open Project of Technology Innovation Center for Spatio-temporal Information and Equipment of Intelligent City (STIEIC-KF202305), the Open Fund of Key Laboratory of Monitoring, Evaluation and Early Warning of Territorial Spatial Planning Implementation, Ministry of Natural Resources (LMEE-KF2023001), Science and Technology Project of Chongqing Municipal Planning and Natural Resources Bureau in 2024 (KJ-2024006), the Open Fund of Key Laboratory of Monitoring, Evaluation and Early Warning of Territorial Spatial Planning Implementation, Ministry of Natural Resources (LMEE-KF2023004), National Key Research and Development Program of China (2023YFC3805303).

Data Availability Statement: The datasets presented in this article are not readily available because the data are part of an ongoing study. Requests to access the datasets should be directed to weima@cqjtu.edu.cn.

Conflicts of Interest: The authors declare no conflicts of interest.

References

1. Gilani, T.A.; Mir, M.S. A study on the assessment of traffic noise induced annoyance and awareness levels about the potential health effects among residents living around a noise-sensitive area. *Environ. Sci. Pollut. Res. Int.* **2021**, *28*, 63045–63064. [CrossRef] [PubMed]
2. Zare Sakhvidi, F.; Zare Sakhvidi, M.J.; Mehrparvar, A.H.; Dzhambov, A.M. Environmental Noise Exposure and Neurodevelopmental and Mental Health Problems in Children: A Systematic Review. *Curr. Environ. Health Rep.* **2018**, *5*, 365–374. [CrossRef] [PubMed]
3. Khomenko, S.; Cirach, M.; Barrera-Gomez, J.; Pereira-Barboza, E.; Iungman, T.; Mueller, N.; Foraster, M.; Tonne, C.; Thondoo, M.; Jephcote, C.; et al. Impact of road traffic noise on annoyance and preventable mortality in European cities: A health impact assessment. *Environ. Int.* **2022**, *162*, 107160. [CrossRef] [PubMed]
4. Hume, K.I.; Brink, M.; Basner, M. Effects of environmental noise on sleep. *Noise Health* **2012**, *14*, 297–302. [CrossRef]
5. Smith, M.G.; Cordoza, M.; Basner, M. Environmental Noise and Effects on Sleep: An Update to the WHO Systematic Review and Meta-Analysis. *Environ. Health Perspect.* **2022**, *130*, 76001. [CrossRef]
6. Babisch, W.; Pershagen, G.; Selander, J.; Houthuijs, D.; Breugelmans, O.; Cadum, E.; Vigna-Taglianti, F.; Katsouyanni, K.; Haralabidis, A.S.; Dimakopoulou, K.; et al. Noise annoyance--a modifier of the association between noise level and cardiovascular health? *Sci. Total Environ.* **2013**, *452–453*, 50–57. [CrossRef]
7. Vienneau, D.; Saucy, A.; Schaffer, B.; Fluckiger, B.; Tangermann, L.; Stafoggia, M.; Wunderli, J.M.; Roosli, M.; SNC Study Group. Transportation noise exposure and cardiovascular mortality: 15-years of follow-up in a nationwide prospective cohort in Switzerland. *Environ. Int.* **2022**, *158*, 106974. [CrossRef]
8. Davri, A.I.; Petropoulos, G.P.; Detsikas, S.E.; Kalogeropoulos, K.; Faka, A. Spatial distribution of noise levels in the Historic Centre of Athens in Greece using geoinformation technologies. In *Geographical Information Science*; Elsevier: Amsterdam, The Netherlands, 2024; pp. 429–454.

9. Tsatsaris, A.; Kalogeropoulos, K.; Stathopoulos, N.; Louka, P.; Tsanakas, K.; Tsesmelis, D.E.; Krassanakis, V.; Petropoulos, G.P.; Pappas, V.; Chalkias, C. Geoinformation Technologies in Support of Environmental Hazards Monitoring under Climate Change: An Extensive Review. *ISPRS Int. J. Geo-Inf.* **2021**, *10*, 94. [CrossRef]
10. Petropoulos, G.P.; Kalivas, D.P.; Georgopoulou, I.A.; Srivastava, P.K. Urban vegetation cover extraction from hyperspectral imagery and geographic information system spatial analysis techniques: Case of Athens, Greece. *J. Appl. Remote Sens.* **2015**, *9*, 096088. [CrossRef]
11. Farcaş, F.; Sivertunb, Å. Road Traffic Noise: GIS Tools for Noise Mapping and a Case Study for Skåne Region. In Proceedings of the ISPRS Workshop on Quality, Scale and Analysis Aspects of City Models, Lund, Sweden, 3–4 December 2009.
12. Debnath, A.; Singh, P.K. Environmental traffic noise modelling of Dhanbad township area—A mathematical based approach. *Appl. Acoust.* **2018**, *129*, 161–172. [CrossRef]
13. Kumar, V.; Ahirwar, A.V.; Prasad, A.D. Monitoring and mapping noise levels of university campus in central part of India. *J. Air Pollut. Health* **2023**, *8*, 1–12. [CrossRef]
14. Almansi, K.Y.; Ujang, U.; Azri, S.; Wickramathilaka, N. Traffic noise prediction model using GIS and ensemble machine learning: A case study at Universiti Teknologi Malaysia (UTM) Campus. *Environ. Sci. Pollut. Res. Int.* **2024**, *31*, 60905–60926. [CrossRef] [PubMed]
15. World Health Organization. *Compendium of WHO and Other UN Guidance on Health and Environment*; World Health Organization: Geneva, Switzerland, 2022.
16. Chen, L.; Tang, B.; Liu, T.; Xiang, H.; Sheng, Q.; Gong, H. Modeling traffic noise in a mountainous city using artificial neural networks and gradient correction. *Transp. Res. Part D Transp. Environ.* **2020**, *78*, 102196. [CrossRef]
17. Xie, D.; Liu, Y.; Chen, J. Mapping urban environmental noise: A land use regression method. *Environ. Sci. Technol.* **2011**, *45*, 7358–7364. [CrossRef]
18. Ibili, F.; Adanu, E.K.; Adams, C.A.; Andam-Akorful, S.A.; Turay, S.S.; Ajayi, S.A. Traffic noise models and noise guidelines: A review. *Noise Vib. Worldw.* **2021**, *53*, 65–79. [CrossRef]
19. Umar, I.K.; Nourani, V.; Gökçekuş, H.; Abba, S.I. An intelligent hybridized computing technique for the prediction of roadway traffic noise in urban environment. *Soft Comput.* **2023**, *27*, 10807–10825. [CrossRef]
20. Umar, I.K.; Gökçekuş, H.; Nourani, V. An intelligent soft computing technique for prediction of vehicular traffic noise. *Arab. J. Geosci.* **2022**, *15*, 1571. [CrossRef]
21. AlKheder, S.; Almutairi, R. Roadway traffic noise modelling in the hot hyper-arid Arabian Gulf region using adaptive neuro-fuzzy interference system. *Transp. Res. Part D Transp. Environ.* **2021**, *97*, 102917. [CrossRef]
22. Nourani, V.; Gokcekus, H.; Umar, I.K. Artificial intelligence based ensemble model for prediction of vehicular traffic noise. *Environ. Res.* **2020**, *180*, 108852. [CrossRef]
23. Navarro, J.M.; Pita, A. Machine Learning Prediction of the Long-Term Environmental Acoustic Pattern of a City Location Using Short-Term Sound Pressure Level Measurements. *Appl. Sci.* **2023**, *13*, 1613. [CrossRef]
24. Alam, P.; Ahmad, K.; Khan, A.H.; Khan, N.A.; Dehghani, M.H. 2D and 3D mapping of traffic induced noise near major roads passing through densely populated residential area of South Delhi, India. *PLoS ONE* **2021**, *16*, e0248939. [CrossRef] [PubMed]
25. Liu, J.; Li, T.; Xie, P.; Du, S.; Teng, F.; Yang, X. Urban big data fusion based on deep learning: An overview. *Inf. Fusion* **2020**, *53*, 123–133. [CrossRef]
26. De Kluijver, H.; Stoter, J. Noise mapping and GIS: Optimising quality and efficiency of noise effect studies. *Comput. Environ. Urban Syst.* **2003**, *27*, 85–102. [CrossRef]
27. Reijnen, R.; Foppen, R.; Veenbaas, G. Disturbance by traffic of breeding birds: Evaluation of the effect and considerations in planning and managing road corridors. *Biodivers. Conserv.* **1997**, *6*, 567–581. [CrossRef]
28. Shim, E.; Kim, D.; Woo, H.; Cho, Y. Designing a Sustainable Noise Mapping System Based on Citizen Scientists Smartphone Sensor Data. *PLoS ONE* **2016**, *11*, e0161835. [CrossRef]
29. Steele, C. A critical review of some traffic noise prediction models. *Appl. Acoust.* **2001**, *62*, 271–287. [CrossRef]
30. Givargis, S.; Mahmoodi, M. Converting the UK calculation of road traffic noise (CORTN) to a model capable of calculating LAeq,1h for the Tehran's roads. *Appl. Acoust.* **2008**, *69*, 1108–1113. [CrossRef]
31. Garg, N.; Maji, S. A critical review of principal traffic noise models: Strategies and implications. *Environ. Impact Assess. Rev.* **2014**, *46*, 68–81. [CrossRef]
32. Yamamoto, K. Road traffic noise prediction model "ASJ RTN-Model 2008": Report of the Research Committee on Road Traffic Noise. *Acoust. Sci. Technol.* **2010**, *31*, 2–55. [CrossRef]
33. Kephalopoulos, S.; Paviotti, M.; Anfosso-Ledee, F.; Van Maercke, D.; Shilton, S.; Jones, N. Advances in the development of common noise assessment methods in Europe: The CNOSSOS-EU framework for strategic environmental noise mapping. *Sci. Total Environ.* **2014**, *482–483*, 400–410. [CrossRef]
34. Dutilleux, G.; Defrance, J.; Ecotière, D.; Gauvreau, B.; Bérengier, M.; Besnard, F.; Duc, E.L. NMPB-Routes-2008: The Revision of the French Method for Road Traffic Noise Prediction. *Acta Acust. United Acust.* **2010**, *96*, 452–462. [CrossRef]

35. *HJ 2.4-2009*; Technical Guidelines for Noise Impact Assessment. State Environmental Protection Administration of China: Beijing, China, 2009.
36. Zhu, L.; Li, X.; Jiang, C.; Liu, L.; Wu, R.; Wang, W.; Zhang, B. Rapid Modeling Method for Road Traffic Noise Sources: A case study in Beijing. *Noise Mapp.* **2015**, *2*, 31–39. [CrossRef]
37. Kumar, P.; Nigam, S.P.; Kumar, N. Vehicular traffic noise modeling using artificial neural network approach. *Transp. Res. Part C Emerg. Technol.* **2014**, *40*, 111–122. [CrossRef]
38. Bravo-Moncayo, L.; Lucio Naranjo, J.; Pavón García, I.; Mosquera, R. Neural based contingent valuation of road traffic noise. *Transp. Res. Part D Transp. Environ.* **2017**, *50*, 26–39. [CrossRef]
39. Hamad, K.; Ali Khalil, M.; Shanableh, A. Modeling roadway traffic noise in a hot climate using artificial neural networks. *Transp. Res. Part D Transp. Environ.* **2017**, *53*, 161–177. [CrossRef]
40. Liu, Y.; Oiamo, T.; Rainham, D.; Chen, H.; Hatzopoulou, M.; Brook, J.R.; Davies, H.; Goudreau, S.; Smargiassi, A. Integrating random forests and propagation models for high-resolution noise mapping. *Environ. Res.* **2021**, *195*, 110905. [CrossRef]
41. Sieber, C.; Ragettli, M.S.; Brink, M.; Toyib, O.; Baatjies, R.; Saucy, A.; Probst-Hensch, N.; Dalvie, M.A.; Roosli, M. Land Use Regression Modeling of Outdoor Noise Exposure in Informal Settlements in Western Cape, South Africa. *Int. J. Environ. Res. Public Health* **2017**, *14*, 1262. [CrossRef]
42. Chang, T.Y.; Liang, C.H.; Wu, C.F.; Chang, L.T. Application of land-use regression models to estimate sound pressure levels and frequency components of road traffic noise in Taichung, Taiwan. *Environ. Int.* **2019**, *131*, 104959. [CrossRef]
43. Xu, X.; Ge, Y.; Wang, W.; Lei, X.; Kan, H.; Cai, J. Application of land use regression to map environmental noise in Shanghai, China. *Environ. Int.* **2022**, *161*, 107111. [CrossRef]
44. Staab, J.; Stark, T.; Wurm, M.; Wolf, K.; Dallavalle, M.; Schady, A.; Lakes, T.; Taubenböck, H. Using CNNs on Sentinel-2 data for road traffic noise modelling. In Proceedings of the 2023 Joint Urban Remote Sensing Event (JURSE), Heraklion, Greece, 17–19 May 2023; pp. 1–4.
45. Tiwari, S.K.; Kumaraswamidhas, L.A.; Gautam, C.; Garg, N. An auto-encoder based LSTM model for prediction of ambient noise levels. *Appl. Acoust.* **2022**, *195*, 108849. [CrossRef]
46. Li, B.; Tao, S.; Dawson, R.W.; Cao, J.; Lam, K. A GIS based road traffic noise prediction model. *Appl. Acoust.* **2002**, *63*, 679–691. [CrossRef]
47. Reed, S.E.; Boggs, J.L.; Mann, J.P. A GIS tool for modeling anthropogenic noise propagation in natural ecosystems. *Environ. Model. Softw.* **2012**, *37*, 1–5. [CrossRef]
48. Gulliver, J.; Morley, D.; Vienneau, D.; Fabbri, F.; Bell, M.; Goodman, P.; Beevers, S.; Dajnak, D.; Kelly, F.J.; Fecht, D. Development of an open-source road traffic noise model for exposure assessment. *Environ. Model. Softw.* **2015**, *74*, 183–193. [CrossRef]
49. Bocher, E.; Guillaume, G.; Picaut, J.; Petit, G.; Fortin, N. NoiseModelling: An Open Source GIS Based Tool to Produce Environmental Noise Maps. *ISPRS Int. J. Geo-Inf.* **2019**, *8*, 130. [CrossRef]
50. Le Bescond, V.; Can, A.; Aumond, P.; Gastineau, P. Open-source modeling chain for the dynamic assessment of road traffic noise exposure. *Transp. Res. Part D Transp. Environ.* **2021**, *94*, 102793. [CrossRef]
51. Liu, Y.; Ma, X.; Boano, C.A. Intelligent Noise Mapping for Smart Cities: Solutions, Trends, and Research Opportunities. *IEEE Commun. Mag.* **2024**, *62*, 18–25. [CrossRef]
52. Ascari, E.; Cerchiai, M.; Gorrasi, P.; Longo, A.; Mencagli, G.; Miccoli, F.; Zappatore, M. OUTFIT: Crowdsourced Data Feeding Noise Maps in Digital Twins. In Proceedings of the 4th Workshop on Flexible Resource and Application Management on the Edge, Pisa, Italy, 3–7 June 2024; pp. 39–46.
53. Barczak, A.; Woźniak, H. Comparative Study on Game Engines. *Stud. Inform.* **2020**, *1*, 5–24. [CrossRef]
54. Soni, L.; Kaur, A. Merits and Demerits of Unreal and Unity: A Comprehensive Comparison. In Proceedings of the 2024 International Conference on Computational Intelligence for Green and Sustainable Technologies (ICCIGST), Vijayawada, India, 18–19 July 2024; pp. 1–5.
55. Stephens, R. Creating an acoustic simulation of the noise pollution affecting a residential area. In Proceedings of the 179th Meeting of the Acoustical Society of America, Virtual, 7–11 December 2020.
56. Khan, J.; Ketzel, M.; Jensen, S.S.; Gulliver, J.; Thysell, E.; Hertel, O. Comparison of Road Traffic Noise prediction models: CNOSSOS-EU, Nord2000 and TRANEX. *Environ. Pollut.* **2021**, *270*, 116240. [CrossRef]
57. Xuan, H.; Li, X. Analysis on CNOSSOS-EU Traffic Noise Prediction Model. *Noise Vib. Control* **2014**, *34*, 269–272. (In Chinese)
58. Gharehchahi, E.; Hashemi, H.; Yunesian, M.; Samaei, M.; Azhdarpoor, A.; Oliaei, M.; Hoseini, M. Geospatial analysis for environmental noise mapping: A land use regression approach in a metropolitan city. *Environ. Res.* **2024**, *257*, 119375. [CrossRef]
59. Al-Shargabi, A.A.; Almhafdy, A.; AlSaleem, S.S.; Berardi, U.; Ali, A.A.M. Optimizing Regression Models for Predicting Noise Pollution Caused by Road Traffic. *Sustainability* **2023**, *15*, 10020. [CrossRef]
60. Tiwari, S.K.; Kumaraswamidhas, L.A.; Prince; Kamal, M.; Rehman, M.U. A hybrid deep leaning model for prediction and parametric sensitivity analysis of noise annoyance. *Environ. Sci. Pollut. Res. Int.* **2023**, *30*, 49666–49684. [CrossRef] [PubMed]

61. Liu, Y.; Goudreau, S.; Oiamo, T.; Rainham, D.; Hatzopoulou, M.; Chen, H.; Davies, H.; Tremblay, M.; Johnson, J.; Bockstael, A.; et al. Comparison of land use regression and random forests models on estimating noise levels in five Canadian cities. *Environ. Pollut.* **2020**, *256*, 113367. [CrossRef] [PubMed]
62. Li, Y.; Wang, S.; Zhang, D. Prediction of Si content of blast furnace hot metal based on data-driven approach. *Baosteel Technol.* **2024**, *6*, 11–16. (In Chinese)
63. McDonald, G.C. Ridge regression. *WIREs Comp. Stat.* **2009**, *1*, 93–100. [CrossRef]
64. Jin, D.; Liu, X. Exploring the carbon emission reduction effects, drivers, and peak carbon strategies in China's energy structure transformation. *J. Saf. Environ.* **2024**, *24*, 4908–4916. (In Chinese)
65. Ragettli, M.S.; Goudreau, S.; Plante, C.; Fournier, M.; Hatzopoulou, M.; Perron, S.; Smargiassi, A. Statistical modeling of the spatial variability of environmental noise levels in Montreal, Canada, using noise measurements and land use characteristics. *J. Expo. Sci. Environ. Epidemiol.* **2016**, *26*, 597–605. [CrossRef]
66. *HJ 640-2012*; Technical Specifications for Environmental Noise Monitoring, Routine Monitoring for Urban Environmental Noise. State Environmental Protection Administration of China: Beijing, China, 2012.

Disclaimer/Publisher's Note: The statements, opinions and data contained in all publications are solely those of the individual author(s) and contributor(s) and not of MDPI and/or the editor(s). MDPI and/or the editor(s) disclaim responsibility for any injury to people or property resulting from any ideas, methods, instructions or products referred to in the content.